Renewable Energy 220 (2024) 119672

Contents lists available at ScienceDirect

Renewable Energy

journal homepage: www.elsevier.com/locate/renene

On the use of reference modules in characterizing the performance of bifacial modules for rooftop canopy applications

Jesús Polo *, Miguel Alonso-Abella, Ana Marcos, Carlos Sanz-Saiz, Nuria Martín-Chivelet

Photovoltaic Solar Energy Unit (Energy Department CIEMAT), Avda. Complutense 40, 28040, Madrid, Spain

ARTICLE INFO

Keywords:
Bifacial PV
Rooftop canopy
PV modeling
Bifacial reference devices
View-factor models

ABSTRACT

The growth of bifacial systems in different photovoltaic (PV) applications is driving new requirements in measuring the effective irradiance for bifacial PV. Non-uniformity of rear irradiance may have a significant impact on the proper characterization of the system. It also has implications on modeling rear irradiance and consequently on performance prediction. In this work, we present a simple way of constructing an irradiance sensor from a commercial bifacial module and the application to performance and rear-side irradiance variability of a small rooftop bifacial PV system is analyzed. In addition, assessment of some commonly used models based on the view-factor approach is performed using as reference the front and rear irradiance simultaneous measurements from the bifacial reference module. The use of bifacial reference modules implies some benefits over arranging calibrated cells for determining rear irradiance, due to their higher field-of-view and representativeness of the response of the system to be monitored. This work also illustrates the high variability of rear irradiance in small systems and the impact of the edge effect. The results here can contribute to a better knowledge of the use of these reference modules as effective irradiance sensors for very bifacial PV configurations.

1. Introduction

Solar photovoltaic (PV) technologies are growing fast in parallel to the impulse towards the reduction of carbon emissions in the energy worldwide context. Therefore, PV power deployment is increasing continuously in different configurations, and some new applications such as rooftop PV or utility-scale floating PV are remarkable in growth now [1]. Additionally, rooftop solar PV is gaining popularity and very different features and technologies are nowadays available to the user [2].

Among PV technologies, bifacial PV is gaining importance very quickly and many new applications based on bifacial systems are being recently proposed. It is suitable for fixed-tilt as well as tracking systems, either in utility-scale, flat roof-top, or integrated installations [3]. A good review of the origins, evolution and testing of bifacial modules can be found in recent literature [4]. Bifacial solar cells increase the power by collecting the light at the rear side, while reducing the area-related costs of PV systems [5]. This feature and the small difference in price with monofacial modules can contribute to minimizing significantly the levelized cost of energy (LCOE) in many applications [6,7]. In fact, PER and nPERT concepts as low-cost Silicon wafers contributed to the expansion of bifacial modules and they are still developing ways to increase the efficiency [3]. Moreover, bifacial PV with single-axis tracking has advantages in improving the temperature sensitivity and gaining energy output [8]. The use of bifacial PV modules in agrivoltaic projects also offers interesting advantages due to the increasing elevations and row spacing [9,10]. Another popular application of bifacial modules is the use of PV modules in carports or canopies [11]. Consequently, bifacial uses and applications are expected to grow notably in the coming years [12].

Bifacial PV modules under real operation can be characterized by the bifacial irradiance factor (BIF), a dimensionless parameter that is used to calculate the effective irradiance reaching the bifacial module, considering the front and rear sides together. The bifacial irradiance factor depends on the in-plane rear side albedo ρ_i and the maximum power bifaciality coefficient φ_{Pmax}, defined as the ratio between rear side and front side I–V characteristic [13].

$$\varphi_{Pmax} = \frac{P_{max,r}}{P_{max,f}} \tag{1}$$

$$BIF = (1 + \varphi_{Pmax}\rho_i), \tag{2}$$

* Corresponding author.
E-mail address: jesus.polo@ciemat.es (J. Polo).

https://doi.org/10.1016/j.renene.2023.119672
Received 26 June 2023; Received in revised form 6 November 2023; Accepted 15 November 2023
Available online 17 November 2023

The efficiency of solar bifacial PV depends on both environmental and design conditions, such as tilt angle, module height and albedo. For instance, albedo ranges around 0.5 can result in an average bifacial gain of 20 %, while grass surfaces have about 5 % of bifacial gain [14]. Therefore, power rating of bifacial systems is challenging because the heterogeneity of the ground usually produces complex and changing shadow patterns. Different testing methods have been proposed for indoor and outdoor conditions [15–17]. The complexity associated with the characterization of the albedo also contributes to the difficulties in modelling bifacial systems [18]. In addition, the rear-side spectral irradiance is affected by the spectral ground albedo so its application to the power rating of bifacial PV is also a topic under study [19,20]. For instance, it has been theoretically estimated that the mismatch of spectral response albedo relative to a bifacial crystalline silicon PV module is around ±3.7 % for a crystalline silicon PV reference cell [19]. In fact, the solar rear irradiance is usually far less uniform than that incoming to the front side, leading thus to mismatch losses [21]. No-uniformity rear irradiance depends on sky conditions and other factors such as the ground material and the number and position of rear irradiance sensors influence the accuracy of the results [22]. The use of many reference cells to measure rear surface irradiance has been proposed for better and more accurate knowledge of the rear irradiance variability [23]. However, reference modules can be used as solar irradiance sensors with some advantages over reference cells [24–29], even for bifacial applications [30]. Monofacial PV module rear oriented has even been proposed as an alternative method for measuring rear irradiance [31]. Experimental comparisons between calibrated reference modules and measurements from small-area sensors (i.e., photodiodes, pyranometers and reference cells) have proven the benefits of the former [32]. In addition, some other methods have proposed the determination of rear irradiance from the operating current of a bifacial module; however, they are limited by the dependence on the inverter's maximum power tracking [33]. Moreover, the International Electrotechnical Commission also recognizes the difficulties in characterizing the rear-side solar irradiance and proposes two options including the possibility of using bifacial reference devices [13]. Therefore, as a result of the literature review, there seems to be still needs for further studies on proper determination of rear irradiance variability and non-uniformity before the establishment of standards [34].

In this work we propose a simple method for converting commercial bifacial modules into solar irradiance sensors able to measure front and rear irradiance at the same time for proper rating of bifacial PV systems. Therefore, we analyze the use of these bifacial reference modules as sensor for measuring at the same time the front and rear irradiance in the characterization and modeling of eight bifacial modules on a rooftop. Two different bifacial reference modules were prepared (TRINA and LG) by dividing the module output into three different electrical signals taken from the junction boxes and installing a shunt resistance to make them work in short-circuit. A multiple layer made of black and white vinyl sheets is used to block the irradiance conveniently at the stripes and allow thus to measure simultaneously front and rear irradiance. Bifacial reference modules have a larger field of view compared to the reference cells and can offer some advantages as solar irradiance sensors for bifacial applications such as having the same spectral response as the modules under test. The main objective in this work is therefore to analyze the applications of bifacial reference modules as irradiance sensor (measuring simultaneously front and rear irradiance) in order to add further contributions and experience to the problem of non-uniformity of rear irradiance in bifacial modules characterization. In particular, we are testing the following features:

- The comparison with the use of several and different calibrated reference cells on the rear side.
- The position of the bifacial reference module in small PV systems to evaluate the impact of edge effects.
- The use of bifacial reference modules in the assessment of bifacial irradiance models based on 2D view factor approach.

The results of this study led to gaining some additional experience and useful knowledge in extending the use of bifacial reference modules to different bifacial PV configurations that might contribute to standardizing the procedures and methods for measuring rear solar irradiance in bifacial PV systems. A simple and effective method for building a sensor of front and rear irradiance with wide field of view from a commercial bifacial module is presented and used in this work, for both evaluating the modeling of output power of bifacial modules and for assessing modeling the rear irradiance. The evaluation of several well-known models for computing rear-side irradiance is performed, thus using the bifacial reference module, showing the different sensitivity and uncertainty of models based on view factor.

2. Experimental facility and bifacial module characterization

Fig. 1 shows the experimental facility used in this work. Eight bifacial modules (four manufactured by LG and four by TRINA) are located on a flat rooftop with a tilt angle of 19° and south-oriented in azimuth. The facility is placed at Ciemat headquarters in Madrid (Spain). The geographic coordinates of the facility are 40.45° N for latitude, and −3.72° E for longitude. I–V curves of each module are monitored by using a multiplexor system that allows the sequential monitoring of the I–V curve of each module with one single tracer. The measurement campaign lasted from November 2022 till May 2023. Many calibrated cells are distributed along the testbench for measuring front and rear solar irradiance: eight reference cells for rear irradiance and five for front irradiance. In addition, two reference bifacial modules (LG and TRINA) are placed on the left side of the middle row to also measure front and rear irradiance simultaneously.

Modules M0 to M7 have been previously measured and characterized according to IEC 60904 for determining the I–V parameters at standard test conditions (STC) using a large-area flash multi-pulsed solar simulator (10 ms of pulse time) and class AAA [35]. Table 1 summarizes some of the main parameters. The bifacial rear irradiance power gain (BiFi) is the slope of the P_{max} versus rear irradiance (G_r) linear fit, and is based on the assumption that the performance of the module at front STC and at any level of rear irradiance can be calculated by interpolation [21].

The calibrated reference bifacial modules (LG and TRINA) result from the transformation of commercial bifacial modules into irradiance sensors. The transformation process consists of the substitution of each of the three bypass diodes by corresponding shunt resistances to allow the measurement of the short-circuit current of each stripe in the module. The short-circuit current is calibrated outdoors to convert the electric signal into solar irradiance measurement. In order to allow the reference module to measure front, rear and total irradiance, layers of opaque vinyl conveniently block the solar cells at each stripe. The central stripe was selected to measure the rear irradiance in order to minimize potential edge effects, and thus the front side of the central stripe was blocked with vinyl. Fig. 2 illustrates, with schemes and pictures, the process of bifacial reference module configured as a solar irradiance detector. Fig. 2 c) shows the shunt resistances in the junction box and Fig. 2 d) shows the reference modules mounted on the outdoor calibration bank. The calibration procedure consists of comparing front and rear sides, sequentially, to an irradiance reference for determining first the calibration constant of the front side, and afterwards repeating the procedure for the calibration constant of the rear side. The third stripe, which is not blocked on either side, remains not calibrated and measures the total short-circuit current of the stripe, generated at both sides. The calibration constants for the front and rear sides of the calibrated reference modules are listed in Table 2. It should be noted that the ratio of the measured calibration constants are, as expected, very consistent with the maximum power bifacial coefficient presented in Table 1. The two bifacial reference modules are placed together (see

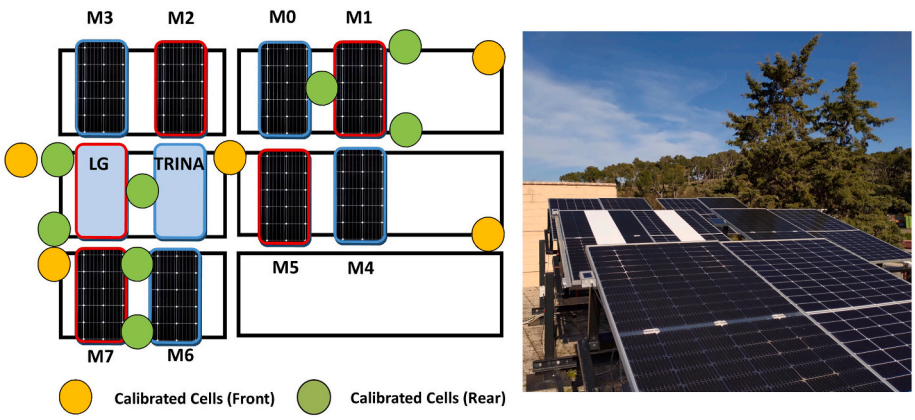

Fig. 1. Scheme and picture of the experimental facility (light blue LG and TRINA refer to calibrated reference modules).

Table 1
Parameters of bifacial PV modules at STC.

Module	Type	P_{max} (W)	BiFi	φ_{Pmax}
M0	TRINA	439	0.2747	0.63
M1	LG	434	0.3288	0.77
M2	LG	433	0.3326	0.77
M3	TRINA	439	0.2717	0.62
M4	TRINA	433	0.2749	0.64
M5	LG	430	0.3310	0.77
M6	TRINA	439	0.2688	0.62
M7	LG	435	0.3320	0.76

Fig. 1) to study the impact of the edge effect on the rear irradiance measured. In addition, the different back cover of LG and TRINA modules might influence in the different sensitivity of rear side calibration constant. In fact, while TRINA uses glass LG have a transparent backsheet of polymeric material. These different materials in the backside might result in slightly different thermal and optical behavior that affect the sensitivity of the rear-side cells.

3. Variability of rear irradiance

Non-homogenous rear irradiance can occur easily in many bifacial applications due to the different sky view factor, non-uniform albedo, complex shadow patterns and edge effects that might occur on the rear side [21,23,30,36]. In the case of the experimental facility under this work the comparison of the different sensors in the middle row (Fig. 1) can illustrate the degree of variability in rear irradiance and the edge effect. Fig. 3 shows the box plot of the hourly mean rear irradiance measured by three calibrated cells (upper left, bottom left and middle right in Fig. 1) and by the reference modules (LG and TRINA). The edge effect is clearly observed in upper and bottom reference cells; since they are placed on the west-side of the facility the boxplot irradiance shows a skewness towards the afternoon. The middle reference cell, placed between LG and TRINA reference modules, is much less sensible to edge effects. The edge effect can also be noticed in the LG reference module, which is placed on the left side; thus, the boxplot of the rear irradiance exhibits some skewness towards the afternoon. Similar situations were observed with the measurements of the sensors placed on the right side

Table 2
Calibration constants for the front and rear sides of the reference modules.

Module	Front side (mV/1000 Wm^{-2})	Rear side (mV/1000 Wm^{-2})
LG	54.08	40.84
TRINA	55.40	35.86

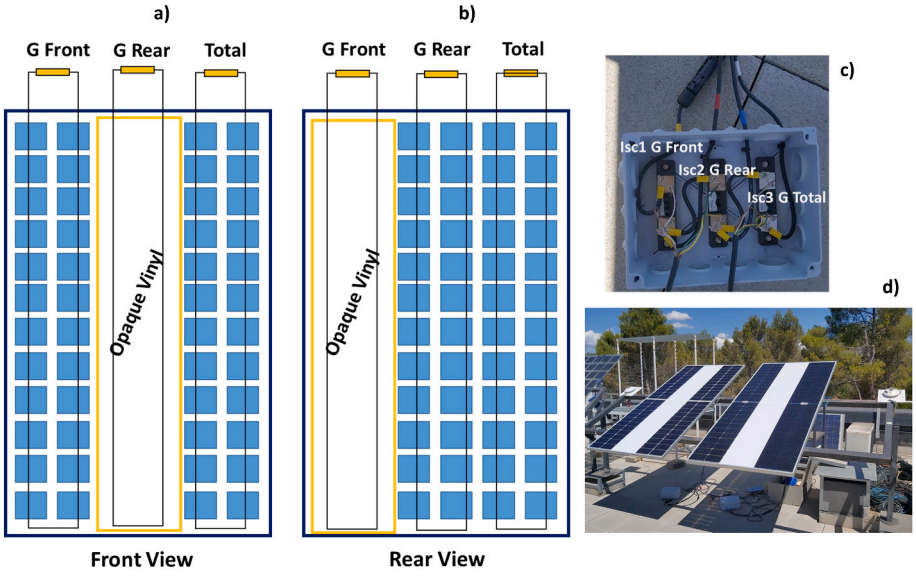

Fig. 2. Bifacial reference modules: a) front view of the scheme; b) rear view of the scheme; c) shunt connections at the bypass diode box; d) outdoor calibration testbench.

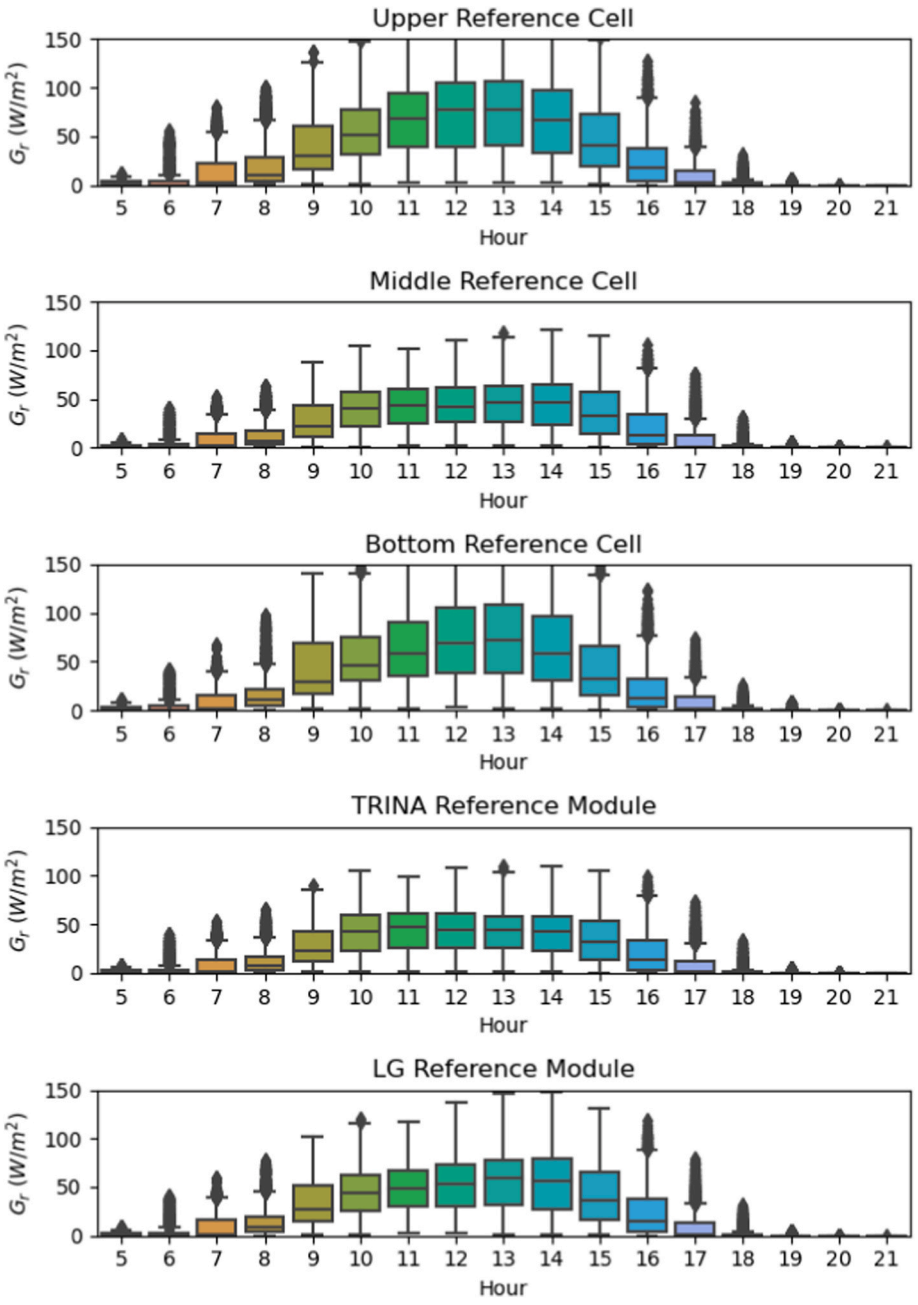

Fig. 3. Boxplot of rear irradiance measured by the different sensors at middle row.

of the upper row (Fig. 1), but in this case, the observed skewness in the hourly rear irradiance moves the mode of the distribution towards the morning.

Variability of the rear irradiance can also be quantified by a parameter named non-uniformity of rear irradiance, defined as [30],

$$GNU = \frac{G_r^{max} - G_r^{min}}{G_r^{max} + G_r^{min}} \tag{3}$$

where G_r^{max} and G_r^{min} are the maximum and minimum values of rear irradiance. GNU, calculated with all the rear irradiance sensors in the testbench during the measuring time, has been placed in the range of 20 %–40 %, being higher when solar radiation is higher, as reported by other works in the same climatic conditions [30]. To illustrate the variability of rear irradiance in the array footprint Fig. 4 shows the heatmaps of the monthly rear irradiation of all sensors. These heatmaps represent the footprint of the experimental facility by a grid of 6 rows and 4 columns; therefore, each module in the facility is represented by one column and two rows. Fig. 4 also shows the boxplot on a monthly basis of the difference between the rear irradiance measured by LG and TRINA reference modules. TRINA reference module is placed in rows 3 and 4, column 2 of the heatmaps shown in Fig. 4. It is the least sensitive to edge effects due to its positioning compared to the other rear sensors. The heatmaps show the impact of the edge effect on the variability of rear irradiance, which is increasing as solar irradiance increases in the spring and early summer months. In addition, the boxplot of the difference between LG and TRINA rear irradiance shows very clearly the higher contribution of the edge effect in the LG reference module, which also increases during the months with higher irradiation.

4. Modeling the performance using bifacial reference modules

Assuming that the TRINA reference module can be used as a good

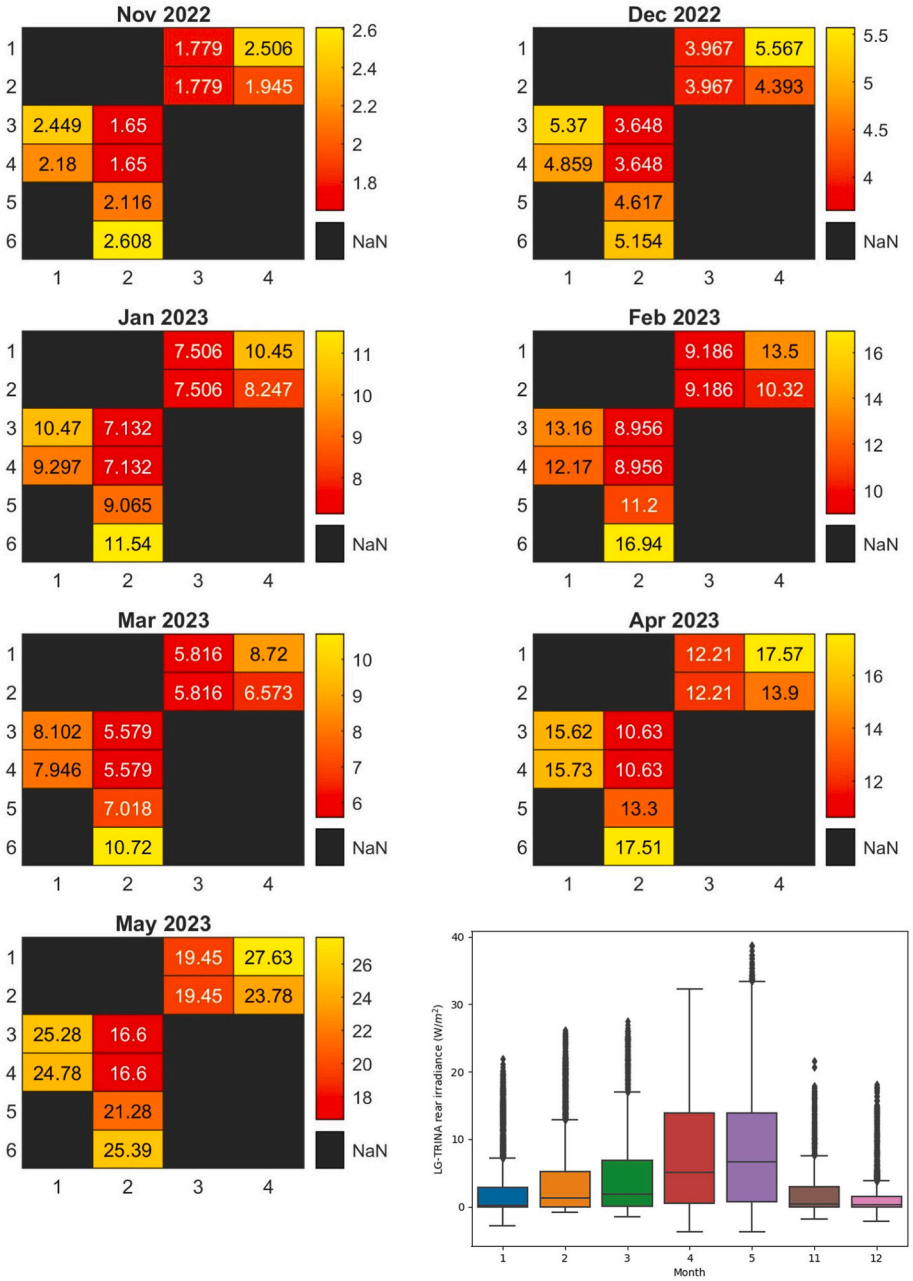

Fig. 4. Monthly rear irradiation measured with the different sensors (kWh m^{-2}) and boxplot of the LG and TRINA rear irradiance difference on a monthly basis.

irradiance sensor for measuring simultaneously both front and rear sides, the irradiance measurements can be used to compute the power output of each bifacial module in the testbench. For that purpose, all the electrical characteristics of the modules given by the manufacturer are coded to modelling each module using pvlib model [37]. The five parameters of the single diode model are computed using the technical parameters of the modules as input. The single diode model included in pvlib is used to compute both the I–V curve and the total power values of each bifacial module by the sum of the front and rear power corresponding to the front and rear effective irradiance [38]. The temperature of the module used as input parameter is the temperature measured at each module by a thermocouple at the rear part of the module. Fig. 5 shows the scatter plot for the eight modules in the testbench and illustrates the sensitivity of each module to the complex irradiance pattern. The effective irradiance used for the frontal and rear sides of the modules was assumed to be the TRINA frontal measurements and the TRINA rear measurements, the latter rated by the bifaciality of each module.

All computing has been performed for the data collected between 10:00 and 14:00 UTC since the modules are placed on a rooftop with some surrounding trees and obstacles, and thus it is ensured no partial shading that might occur in the morning and afternoon. The modelling results are more accurate for the modules closer to the TRINA reference module (M5, M4, M2, M6 and M7). Table 3 shows error metrics for this modelling, which are in the range of 6–16 W m^{-2} (mean absolute error).

The performance ratio for bifacial modules (PR_{bi}) is computed through the following equation [13],

$$PR_{bi} = \frac{P_{out}}{\left(P_{max} G_f BIF\right)/G_{ref}} \tag{4}$$

Where P_{out} is the power output, P_{max} is the nominal power of the module (Table 1), G_f is the front irradiance, G_{ref} is the reference irradiance (1000 W m^{-2}), and *BIF* is the bifacial irradiance factor, defined in Equation (2).

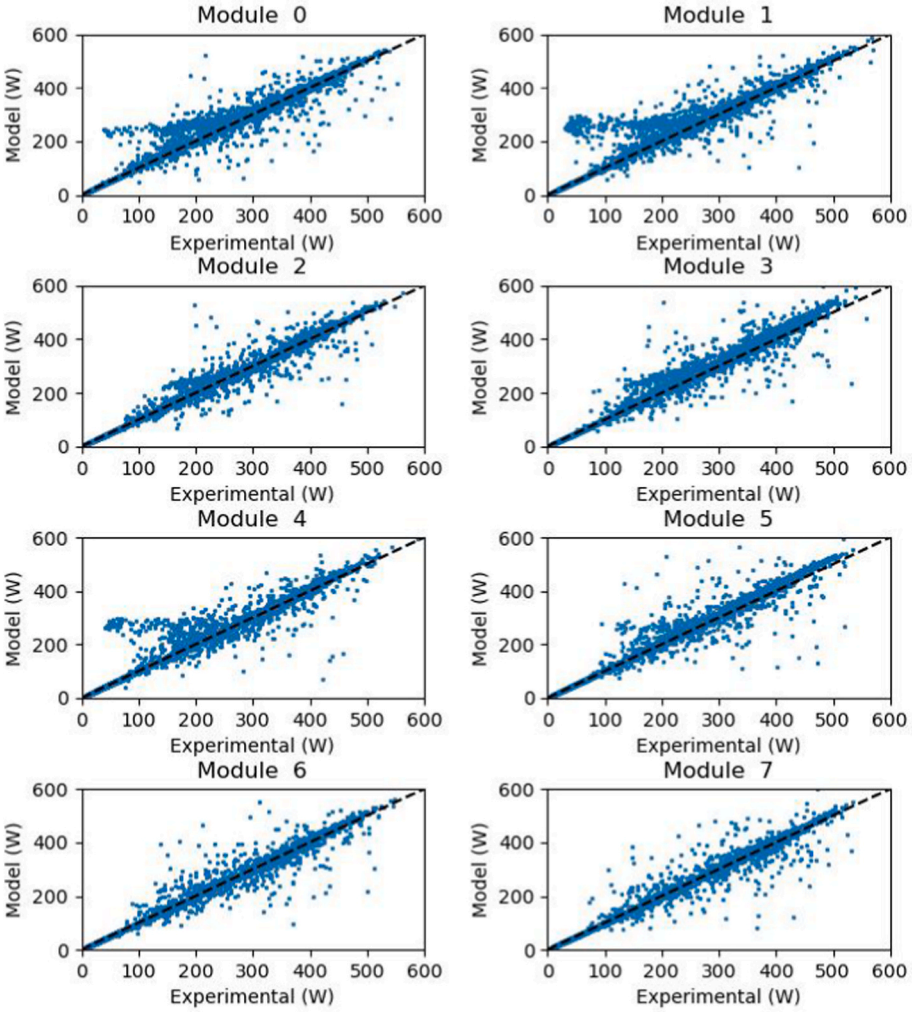

Fig. 5. Scatter plots of the computation of bifacial modules power output.

Table 3
Metrics of modelling bifacial power with reference module.

Module	MAE (W m^{-2})	RMSE (W m^{-2})	R^2
M0	12.3	25.9	0.96
M1	12.3	31.2	0.95
M2	8.1	17.7	0.98
M3	16.1	25.4	0.96
M4	9.1	25.5	0.96
M5	12.3	22.7	0.97
M6	6.7	17.6	0.98
M7	6.8	17.6	0.98

Thus, the performance ratio of all the bifacial modules in the test-bench has been calculated for the interval time between 10:00 and 14:00 UTC using the irradiance measured with the TRINA reference module. The monthly average performance ratio is shown in Fig. 6. In spring and early summer, the performance ratio of all the modules converges as the sun elevation is higher and the edge effects contribution is much lower.

To estimate the bifacial gain, a monofacial module Yingli YL265P-29b was installed for three weeks in the bottom row, next to M6 module. The measured nominal power of the monofacial module was 263.4 W. Since the modules are different in power, the determination of the bifacial gain (BG) was performed with the comparison of power values normalized by the corresponding nominal powers,

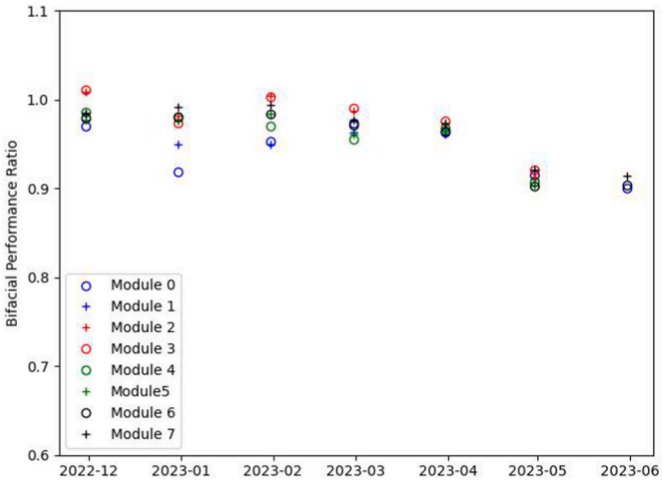

Fig. 6. Performance ratio of the bifacial modules.

$$BG = \frac{P_{bi}/P_{bi,STC} - P_{mo}/P_{mo,STC}}{P_{mo}/P_{mo,STC}} \quad (5)$$

Where the subscript *bi* and *mo* refers to bifacial and monofacial, respectively. Average bifacial gains estimated for modules M6 and M7 were 14 % and 21 %, respectively. The higher bifacial gain of M7 (LG) compared to M6 (TRINA) is associated to the higher bifaciality factor of LG and to the higher impact of edge effects in LG bifacial module due to its positioning in the testbench.

5. Application of bifacial irradiance models

Models for computing back and front surface irradiance for bifacial applications can be grouped into three categories: ray-tracing models, view factor approaches and empirical models [39]. View factor based models calculate the fraction of irradiance scattered or reflected from the surroundings. They estimate the diffuse, direct beam and ground-reflected irradiance for the rear side of the module taking into account the view factor. The view factor, in this context, is the fraction of the radiation from a given surface (collection of surrounding surfaces near the array) that hits the back side of the row of bifacial modules. View factor models can be implemented easily but they might be not accurate enough with irregular geometries and structures. The front side irradiance is computed by the sum of the direct, sky diffuse and reflected contributions. The rear side is essentially similar, taking into account the angle of incidence on the back side and the view factor of the rear surface. The models used here belong to the 2D view factor category, which assumes the length of the module rows to be infinite. Thus, geometric parameters as the ground clearance ratio (ratio between the PV module area and the total ground area), row height or tilt angle, and physical parameters such as the albedo are the main input together with the basic solar irradiance components (direct normal and diffuse horizontal irradiance).

Bifacial irradiance models based on the 2D view factor concept are simple and very fast in computing compared to ray-tracing models. However, as they usually assume infinite row extent, they might underestimate the edge effects in small-size systems. Three bifacial irradiance models have been used here to compute front and rear irradiance corresponding to the TRINA bifacial reference module: Purdue [6,40], pvfactors [41] and biacialVF model [42], all of them available in pvlib or github repository. Bifacial VF is also the model implemented in System Advisor Model (SAM) which is a very powerful and popular tool for modeling solar power systems [43]. Bifacial VF assumes a 5-row PV system of infinite extent and returns the irradiance profile along the middle row.

In order to run the bifacial irradiance models we need measurements of the basic components of solar radiation, diffuse horizontal (DHI) and direct normal (DNI) irradiances. A complete solar radiation station is placed on the rooftop adjacent to the testbench rooftop. Kipp & Zonen CM11 pyranometers were used for measuring global and diffuse horizontal irradiances, and a first class pyrheliometer was used to measure the direct normal irradiance. Measurements of DNI, DHI and global horizontal irradiance (GHI) have been analyzed in quality following the

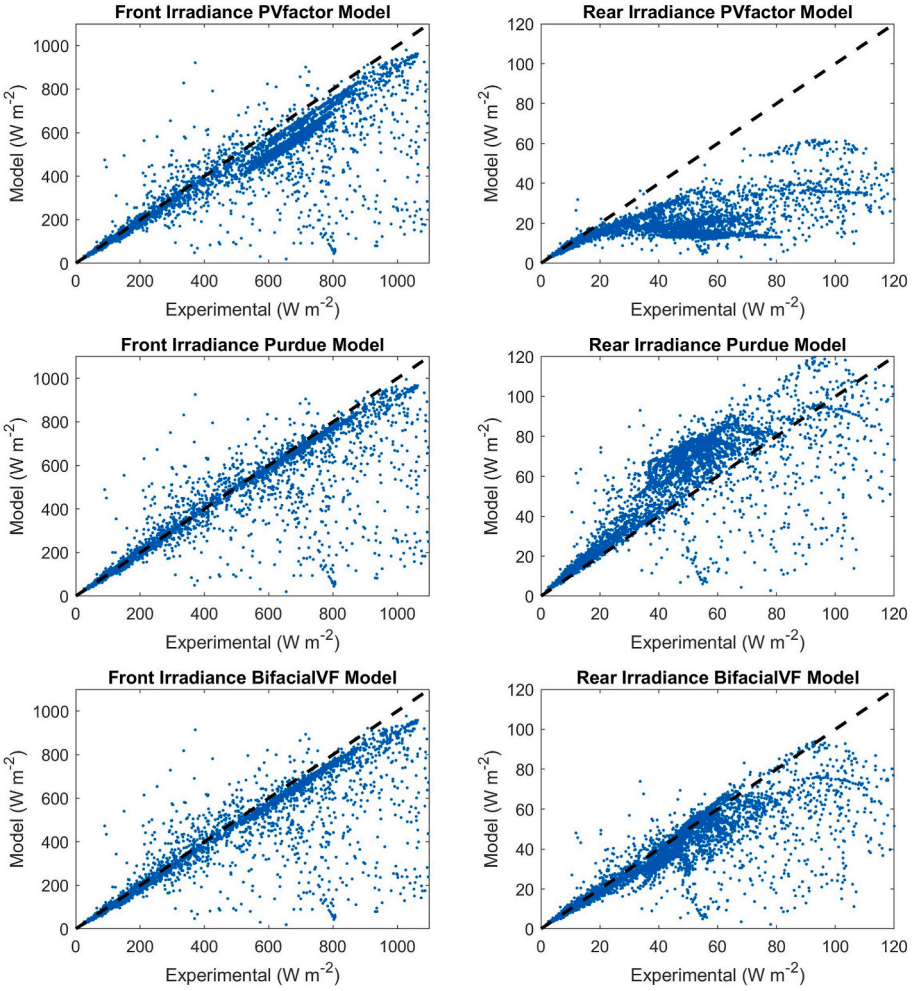

Fig. 7. Scatter plots of bifacial irradiance models based on view factor approach.

Long and Dutton test recommended by the BSRN (Baseline of Surface Radiation Network). Only those measurements that have passed the quality check limits were used as input for bifacial irradiance models [44]. Fig. 7 shows the scatter plot corresponding to the front and rear irradiance estimated by the three bifacial irradiance models tested. Significant dispersion is observed in rear irradiance due to the complexity of modeling the variability, in part due probably to the fact that they cannot model edge effects properly. These models assume large strings of PV modules. Purdue model tends to overestimate the rear irradiance, while the other two tend to underestimate it. BifacialVF is the model that best performs both front and rear irradiance measured by the TRINA reference module. The mean absolute error for rear irradiance are 18.2, 20.0 and 6.9 Wm^{-2} for Purdue, pvfactor and BifacialVF models, respectively. In the case of front irradiance, the mean absolute errors were 72.9, 103.4 and 81.0 Wm^{-2}. It should be noted that the irradiance station is not placed just at the same rooftop as the testbench but on the adjacent one. In consequence, part of the uncertainty of the bifacial irradiance models comes from the uncertainty in the solar radiation components. Nevertheless, and despite the complexity of this comparison the BifacialVF model accuracy is remarkable.

6. Conclusions

Bifacial PV systems are growing in parallel to the increasing applications where bifaciality may offer advantages. Carport and other canopies, noise barriers, agrivoltaic or PV power plants with single-axis tracking are some of the examples of bifacial PV configurations. However, bifaciality produces complexity in the rating and characterization of many bifacial systems due to the non-uniformity of rear irradiance. Complex albedo and partial shadowing from the different surfaces and structures challenges the proper characterization of bifacial systems and lead to mismatch loses in the systems. In this context, different approaches to measure rear-side irradiance are being proposed in the community. On the other hand, in modelling bifacial systems, and particularly in modelling rear irradiance, several approaches and efforts have led to the availability of open source models (ray-tracing ad view-factor based) that are very useful in designing and deploying new systems. However, there are still challenging features associated to some input parameters, such as the complex variability of the albedo. Therefore, there is no standard yet for measuring rear irradiance for rating bifacial systems, and further research is needed to extend the cumulative experience.

In measuring the in-plane irradiance for bifacial systems the use of bifacial reference devices has the benefit of permitting simultaneous measurements of front and rear irradiance with one single instrument, and at the same time it has identical response as the modules to be monitored. In this work we have studied the use of bifacial reference modules on a small rooftop system with eight modules. We describe a simple method for building bifacial reference modules, which were prepared and calibrated to measure front and rear irradiance. Rear irradiance is then measured by bifacial reference modules and with eight reference cells, which were distributed along the system to also analyze the non-uniformity of rear irradiance. The variability of rear irradiance is significant in small systems as the one under study here. Bifacial reference modules can be a good solution for monitoring the front and rear effective irradiance in bifacial PV systems since they have a larger field-of-view than calibrated cells, and they capture the edge effect. The latter would require several calibrated cells, which complicates the data processing. However, it is recommended to place the bifacial reference sensors on the same array racking as the modules under testing and guarantee they have a representative field of view.

In this work we have also explored the use of three view-factor based models for computing front and rear irradiance. The assessment of the modelling has been done by comparison to the bifacial reference module measurements of front and rear irradiance. Uncertainty in the rear irradiance estimation is usually high since both the uncertainty in the inputs, albedo and the basic components of the solar radiation (direct normal and diffuse horizontal), may enhance the model characteristic uncertainties.

In future work, a thorough study on the sensitivity of the bifacial reference modules to the position and to different ground conditions is planned in order to better characterize the possible uses of these devices as sensors for bifacial systems. In addition, other PV technologies (such as Heterojunction Technologies) will be explored to evaluate the potential benefits of higher bifaciality in measuring the rear side irradiance.

Declaration of competing interest

The authors declare that they have no known competing financial interests or personal relationships that could have appeared to influence the work reported in this paper.

Acknowledgements

The authors would like to thank the RINGS-BIPV (Advanced Modeling and Prediction of BIPV) Project (PID2021-124910OB-C31), which is funded by the Spanish Ministerio de Ciencia e Innovación.

References

[1] International Energy Agency(IEA), Snapshot of Global PV Markets 2023, 2023. http://www.iea-pvps.org/fileadmin/dam/public/report/technical/PVPS_report_-_A_Snapshot_of_Global_PV_-_1992-2014.pdf.
[2] J. Abreu, N. Wingartz, N. Hardy, New trends in solar: a comparative study assessing the attitudes towards the adoption of rooftop PV, Energy Pol. 128 (2019) 347–363, https://doi.org/10.1016/J.ENPOL.2018.12.038.
[3] R. Kopecek, J. Libal, Bifacial photovoltaics 2021: status, opportunities and challenges, Energies 14 (2021), https://doi.org/10.3390/en14082076.
[4] J. Eguren, F. Martínez-Moreno, P. Merodio, E. Lorenzo, First bifacial PV modules early 1983, Sol. Energy 243 (2022) 327–335, https://doi.org/10.1016/J.SOLENER.2022.08.002.
[5] R. Guerrero-Lemus, R. Vega, T. Kim, A. Kimm, L.E. Shephard, Bifacial solar photovoltaics – a technology review, Renew. Sustain. Energy Rev. 60 (2016) 1533–1549, https://doi.org/10.1016/J.RSER.2016.03.041.
[6] X. Sun, M.R. Khan, C. Deline, M.A. Alam, Optimization and performance of bifacial solar modules: a global perspective, Appl. Energy 212 (2018) 1601–1610, https://doi.org/10.1016/j.apenergy.2017.12.041.
[7] M.T. Patel, M.R. Khan, X. Sun, M.A. Alam, A worldwide cost-based design and optimization of tilted bifacial solar farms, Appl. Energy 247 (2019) 467–479, https://doi.org/10.1016/J.APENERGY.2019.03.150.
[8] M.T. Patel, M.S. Ahmed, H. Imran, N.Z. Butt, M.R. Khan, M.A. Alam, Global analysis of next-generation utility-scale PV: tracking bifacial solar farms, Appl. Energy 290 (2021), 116478, https://doi.org/10.1016/J.APENERGY.2021.116478.
[9] O.A. Katsikogiannis, H. Ziar, O. Isabella, Integration of bifacial photovoltaics in agrivoltaic systems: a synergistic design approach, Appl. Energy 309 (2022), 118475, https://doi.org/10.1016/J.APENERGY.2021.118475.
[10] E. Mouhib, L. Micheli, F.M. Almonacid, E.F. Fernández, E. Mouhib, L. Micheli, F. M. Almonacid, E.F. Fernández, Overview of the fundamentals and applications of bifacial photovoltaic technology: agrivoltaics and aquavoltaics, Energies 15 (2022), https://doi.org/10.3390/EN15238777.
[11] S. Hwang, H. seok Lee, Y. Kang, Energy yield comparison between monofacial photovoltaic modules with monofacial and bifacial cells in a carport, Energy Rep. 9 (2023) 3148–3153, https://doi.org/10.1016/J.EGYR.2023.02.011.
[12] G. Raina, S. Sinha, A holistic review approach of design considerations, modelling, challenges and future applications for bifacial photovoltaics, Energy Convers. Manag. 271 (2022), 116290, https://doi.org/10.1016/J.ENCONMAN.2022.116290.
[13] IEC 61724-1, Photovoltaic System Performance – Part 1: Monitoring, 2021. IEC 61724-1 ED2.
[14] K. Ganesan, D.P. Winston, S. Sugumar, S. Jegan, Performance analysis of n-type PERT bifacial solar PV module under diverse albedo conditions, Sol. Energy 252 (2023) 81–90, https://doi.org/10.1016/J.SOLENER.2023.01.020.
[15] J. Lopez-garcia, B. Haile, D. Pavanello, A. Pozza, T. Sample, Characterisation of n-type bifacial silicon PV modules, 32nd, Eur. Photovolt. Sol. Energy Conf. Exhib. (2016) 1724–1729.
[16] J. Lopez-Garcia, A. Casado, T. Sample, Electrical performance of bifacial silicon PV modules under different indoor mounting configurations affecting the rear reflected irradiance, Sol. Energy 177 (2019) 471–482, https://doi.org/10.1016/J.SOLENER.2018.11.051.
[17] B.K. Newman, A. Carr, K. de Groot, N. Dekker, B. van Aken, A. Vlooswijk, B. van de Loo, Comparison of bifacial laboratory testing methods, in: Eur. PV Sol. Energy Conf. Exhib. EU PVSEC, 2017, pp. 2–5, 25-27 September 2017, Amsterdan.

[18] C.A. Gueymard, V. Lara-Fanego, M. Sengupta, Y. Xie, Surface albedo and reflectance: review of definitions, angular and spectral effects, and intercomparison of major data sources in support of advanced solar irradiance modeling over the Americas, Sol. Energy 182 (2019) 194–212, https://doi.org/10.1016/j.solener.2019.02.040.

[19] M. Gostein, B. Marion, B. Stueve, Spectral effects in albedo and rearside irradiance measurement for bifacial performance estimation, Conf. Rec. IEEE Photovolt. Spec. Conf. (2020-June), https://doi.org/10.1109/PVSC45281.2020.9300518, 2020) 0515–0519.

[20] C. Monokroussos, Q. Gao, X.Y. Zhang, E. Lee, Y. Wang, C. Zou, L. Rimmelspacher, J.B. Castro, M. Schweiger, W. Herrmann, Rear-side spectral irradiance at 1 sun and application to bifacial module power rating, Prog. Photovoltaics Res. Appl. 28 (2020) 755–766, https://doi.org/10.1002/pip.3268.

[21] J.S. Stein, C. Reise, J.B. Castro, G. Friesen, G. Maugeri, E. Urrejola, S. Ranta, Bifacial PV Modules & Systems Experience and Results from International Research and Pilot Applications, 2021.

[22] E. Ozkalay, J. López-García, L. Pinedo-Prieto, A.M. Gracia-Amillo, R.P. Kenny, Evaluation of the non-uniformity of rear-side irradiance in, in: SiliconPV 2019, 9TH Int. Conf. Cryst. SILICON PHOTOVOLTAICS, 2019, https://doi.org/10.1063/1.5123816, 8-10 April 2019, Leuven, Belgium.

[23] C.W. Hansen, R. Gooding, N. Guay, D.M. Riley, J. Kallickal, A. Asgharzadeh, B. Marion, F. Toor, J.S. Stein, A detailed model of rear-side irradiance for bifacial PV modules, in: 44th IEEE Photovolt. Spec. Conf., 2017, pp. SAND2017–6464C. Washington, DC.

[24] J. Polo, W.G. Fernandez-Neira, M.C. Alonso-García, On the use of reference modules as irradiance sensor for monitoring and modelling rooftop PV systems, Renew. Energy 106 (2017) 186–191, https://doi.org/10.1016/j.renene.2017.01.026.

[25] F. Martínez-Moreno, E. Lorenzo, J. Muñoz, R. Moretón, On the testing of large PV arrays, Prog. Photovoltaics Res. Appl. 20 (2012) 100–105, https://doi.org/10.1002/pip.1102.

[26] M. Gostein, S.A. Pelaez, C. Deline, A. Habte, C.W. Hansen, B. Marion, J. Newmiller, M. Sengupta, J.S. Stein, I. Suez, Measuring irradiance for bifacial PV systems, Conf. Rec. IEEE Photovolt. Spec. Conf. (2021) 896–903, https://doi.org/10.1109/PVSC43889.2021.9518601.

[27] J.L. Braid, J.S. Stein, B.H. King, C. Raupp, J. Mallineni, J. Robinson, S. Knapp, Effective irradiance monitoring using reference modules, in: 2022 IEEE 49th Photovoltaics Spec. Conf., 2022, pp. 1073–1078, https://doi.org/10.1109/PVSC48317.2022.9938851.

[28] S.E. Fahlman, Faster-learning Variations on Back-Propagation: an Empirical Study, in: D. Touretzky, G. Hinton, T. Sejnowski (Eds.), Carnegic Mellon University, n.d.: pp. 38–51.

[29] Y. Hishikawa, M. Higa, T. Takenouchi, Y. Ueda, K. Nishioka, T. Kobayashi, T. Minemoto, H. Taniguchi, H. Wakabayashi, M. Yoshita, Improved precision of the outdoor performance measurements of photovoltaic modules by using the photovoltaic irradiance sensor, Sol. Energy 211 (2020) 82–89, https://doi.org/10.1016/J.SOLENER.2020.09.002.

[30] J.R. Ledesma, R.H. Almeida, F. Martinez-Moreno, C. Rossa, J. Martín-Rueda, L. Narvarte, E. Lorenzo, A simulation model of the irradiation and energy yield of large bifacial photovoltaic plants, Sol. Energy 206 (2020) 522–538, https://doi.org/10.1016/j.solener.2020.05.108.

[31] M. Aghaei, M. Korevaar, P. Babal, H. Ziar, Bifacial photovoltaic technology: recent advancements, simulation and performance measurement, in: M. Aghaei (Ed.), Sol. Radiat., 2022, https://doi.org/10.5772/intechopen.105152. IntechOpen, Rijeka.

[32] N. Riedel-Lyngskar, M. Bartholomaus, J. Vedde, P.B. Poulsen, S. Spataru, Measuring irradiance with bifacial reference panels, IEEE J. Photovoltaics 12 (2022) 1324–1333, https://doi.org/10.1109/JPHOTOV.2022.3201468.

[33] C.F. Abe, J. Batista Dias, G. Notton, G.A. Faggianelli, G. Pigelet, D. Ouvrard, Estimation of the effective irradiance and bifacial gain for PV arrays using the maximum power current, IEEE J. Photovoltaics 13 (2023) 432–441, https://doi.org/10.1109/JPHOTOV.2023.3242117.

[34] P. Babal, M. Korevaar, S. Franken, J. Mes, T. Bergmans, K. Wilson, Uncertainties in irradiance measurements of sensors to POArear of bifacial solar panels, in: 2020 47th IEEE Photovolt. Spec. Conf., 2020, pp. 959–963, https://doi.org/10.1109/PVSC45281.2020.9301008.

[35] IEC 60904, Photovoltaic Devices – Part 1-2: Measurement of Current-Voltage Characteristics of Bifacial Photovoltaic (PV) Devices, 2023.

[36] B. Durusoy, T. Ozden, B.G. Akinoglu, Solar irradiation on the rear surface of bifacial solar modules: a modeling approach, Sci. Rep. 10 (2020) 1–10, https://doi.org/10.1038/s41598-020-70235-3.

[37] W.F. Holmgren, C.H. Hansen, M.A. Mikofski, Pvlib Python: a Python package for modeling solar energy systems, J. Open Source Softw. 3 (2018) 884, https://doi.org/10.21105/joss.00884.

[38] A. Jain, Exact analytical solutions of the parameters of real solar cells using Lambert W-function, Sol. Energy Mater. Sol. Cells 81 (2004) 269–277, https://doi.org/10.1016/j.solmat.2003.11.018.

[39] S. Ayala-Pelaez, C. Deline, S.M. Macalpine, B. Marion, J.S. Stein, R.K. Kostuk, Comparison of bifacial solar irradiance model predictions with field validation, IEEE J. Photovoltaics 9 (2019) 82–88, https://doi.org/10.1109/JPHOTOV.2018.2877000.

[40] M.R. Khan, A. Hanna, X. Sun, M.A. Alam, M. Ryyan Khan, A. Hanna, X. Sun, M. A. Alam, Vertical bifacial solar farms: physics, design, and global optimization, Appl. Energy 206 (2017) 240–248, https://doi.org/10.1016/j.apenergy.2017.08.042.

[41] M.A. Anoma, D. Jacob, B.C. Bourne, J.A. Scholl, D.M. Riley, C.W. Hansen, View factor model and validation for bifacial PV and diffuse shade on single-Axis trackers, in: 44th IEEE Photovolt. Spec. Conf., 2017, pp. 1549–1554, https://doi.org/10.1109/pvsc.2017.8366704.

[42] B. Marion, S. Macalpine, C.D. Nrel, A practical irradiance model for bifacial PV modules, in: 44th IEEE Photovolt. Spec. Conf., 2017. Washington, DC. SAND2017-6464C.

[43] N. Blair, N. Diorio, J. Freeman, P. Gilman, S. Janzou, T. Neises, M. Wagner, N. Blair, N. Diorio, J. Freeman, P. Gilman, S. Janzou, T. Neises, M. Wagner, System Advisor Model (SAM) General Description, 2018, https://doi.org/10.1111/j.1532-5415.2009.02342.x. Version 2017.9.5), Golden (CO).

[44] A. Forstinger, S. Wilbert, A.R. Jensen, B. Kraas, C. Fernández-Peruchena, C. Gueymard, D. Ronzio, D. Yang, E. Colino, J. Polo, J.A. Ruiz-Arias, N. Hanrieder, P. Blanc, Y.-M. Saint-Drenan, Expert quality control of solar radiation ground data sets, in: SWC 2021 ISES Sol. World Congr. - Int. Sol. Energy Soc., 2021, https://doi.org/10.18086/swc.2021.38.02.